J. Am. Soc. Mass Spectrom. (2019) 30:634–638
DOI: 10.1007/s13361-018-2119-3

RESEARCH ARTICLE

Laser Ablation Generation of Antimony Selenide Clusters: Laser Desorption Ionization (LDI) Quadrupole Ion Trap Time of Flight Mass Spectrometry

Fei Huang,[1] Lubomír Prokeš,[1,2,3] Josef Havel[1]

[1]Department of Chemistry, Faculty of Science, Masaryk University, Kamenice 5/A14, 62500, Brno, Czech Republic
[2]Department of Physical Electronics, Faculty of Science, Masaryk University, Kotlářská 2, 61137, Brno, Czech Republic
[3]CEPLANT, R&D Centre for Low-Cost Plasma and Nanotechnology Surface Modification, Masaryk University, Kotlářská 2, 61137, Brno, Czech Republic

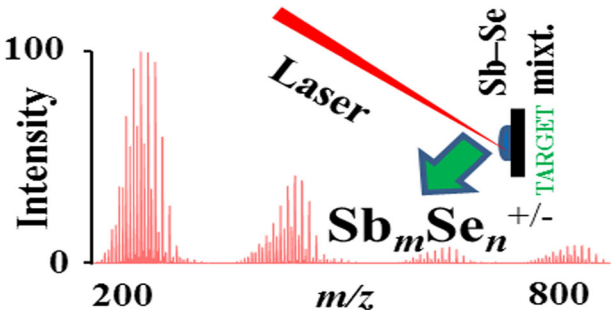

Abstract. The binary system Sb-Se was studied via laser ablation using antimony-selenium mixtures made from powdered elements in various ratios generating new Sb_mSe_n clusters. The results show that in addition to Sb_m^+ ($m = 1–8$) and Se_n^+ ($n = 2–9$) clusters, a series of $Sb_mSe_n^+$ clusters such as $SbSe_{1–8}^+$, $Sb_2Se_{1–6}^+$, $Sb_3Se_{1–5}^+$, $Sb_4Se_{1–3}^+$, and $Sb_5Se_{1,2}^+$ is generated. In addition, some low intensity oxidized clusters like $Se_6O_2^+$, $Se_7O_2^+$, and $SbSe_{2-6}O_5^+$ and partially hydroxylated clusters ($SbSeO_2H_7^+$, $SbSe_5O_4H^+$) are also formed. In total, 24 new antimony selenide clusters were generated. The knowledge gained can contribute to the elucidation of the structure of Sb_mSe_n glasses.

Keywords: Antimony selenides, Laser ablation, Clusters, Laser desorption ionization, Quadrupole ion trap mass spectrometry, Chalcogenide glasses

Received: 15 August 2018/Revised: 5 December 2018/Accepted: 10 December 2018/Published Online: 15 January 2019

Introduction

Antimony forms several selenides. The structure of Sb_2Se_3 has been determined [1–4]. Recently, polycyclic polycations $[Sb_{10}Se_{10}]^{2+}$, $[Sb_7Se_8Br_2]^{3+}$ and $[Sb_{13}Se_{16}Br_2]^{5+}$ [5, 6], $Ba_2Sb_2Se_5$, and $Ba_6Sb_7Se_{16}$ compounds [7] and a huge $Sb_{12}Se_{20}^{4-}$ zintl anion [8] have been prepared and characterized. Antimony-selenium glasses are important members of the chalcogenide range of glasses, especially Ge-As(Te)-Sb-Se. Ge-Sb-Se moldable compounds are used in infrared optics [9–11].

In this work, the binary system Sb-Se was studied via laser ablation generating Sb_mSe_n clusters, in both positive and negative ion modes, using antimony-selenium powdered mixtures in various ratios as precursors. Laser ablation generation with quadrupole ion trap time-of-flight mass spectrometry (QIT-TOFMS) has already been shown to be an important and powerful methodology for studying the formation of clusters [12]; while the composition of Sb_mSe_n clusters was determined via computer simulation of the isotopic envelopes.

Experimental

Chemicals

1-Butyl-3-methylimidazolium chloride, antimony, and selenium powders were purchased from Sigma-Aldrich (St. Louis, Mo., USA). Glycerol and xylene were purchased from Lach-Ner (Neratovice, Czech Republic). *Parafilm* was purchased from Bemis NA (Neenah, Wis., USA). Acetonitrile and hydrochloric acid were purchased from Sigma-Aldrich (Steinheim, Germany). Red phosphorus was obtained from Riedel de Haën (Hannover, Germany) and was purified via sublimation in a nitrogen atmosphere. Water was double distilled using a quartz

Electronic supplementary material The online version of this article (https://doi.org/10.1007/s13361-018-2119-3) contains supplementary material, which is available to authorized users.

Correspondence to: Josef Havel; *e-mail:* havel@chemi.muni.cz

apparatus from Heraeus Quarzschmelze (Hanau, Germany). All other reagents were of analytical grade purity.

Mass Spectrometry

Mass spectra were recorded in both positive and negative ion modes using the mass spectrometer AXIMA Resonance from Kratos Analytical Ltd. (Manchester, UK) coupled with a quadrupole ion trap and time-of-flight detection. The instrument was equipped with a nitrogen laser (337 nm). The laser repetition rate was set to 5 Hz with a pulse time width of 3 ns.

Software and Computation

Stoichiometry of Sb_mSe_n clusters was determined via computer modeling of the isotopic envelopes using Launchpad software (Kompact version 2.9.3, 2011) from Kratos Analytical Ltd. (Manchester, UK).

Sample Preparation for Mass Spectrometry

The surface of solid antimony in pellets was cleaned by applying 0.1 M hydrochloric acid for 5 min. The pellets were then washed with double-distilled water and acetonitrile. Solid antimony was then powdered in an agate mortar. Finally, antimony, selenium, and antimony-selenium mixtures were suspended in acetonitrile (1 mg/ml). From these suspensions, 10 μL was deposited on a target and dried.

For laser ablation in glycerol a 10-μL sample of the Sb-Se suspension in acetonitrile was deposited on a target and dried as mentioned above. After adding 10-μL glycerol, the sample for laser ablation in glycerol was obtained.

For laser ablation generation in mixture of paraffines, 1 cm^2 of parafilm was dissolved in 1 ml of xylene, and then the powdered mixture of antimony-selenium (1 mg) was suspended in this solution. Then, about 1 μL of the suspension was deposited on a target. After drying, the mass spectra were generated.

For laser ablation generation in ionic liquid, the powdered Sb-Se mixture was mixed with an ionic liquid (1-butyl-3-methyl imidazolium chloride), dissolved in acetonitrile, and ~ 1 μL of the suspension was deposited onto a target and dried.

Results

Antimony, selenium, and antimony-selenium clusters generated via laser ablation were studied. A reflectron mode was employed to record the mass spectra in both positive and negative ion modes. It was shown that many more clusters were generated in positive ion mode and the clusters produced in negative ion mode were of low intensity. The results will therefore be presented mainly for the positive ion mode. The majority of the clusters were formed in the *m/z* range of 200–800.

Antimony and Selenium

The overview of clusters generated from antimony and selenium is given in Table 1. Apart from Sb_m^+ ($m = 1$–6) and Se_n^+ ($n = 2$–9) clusters, several oxygen containing clusters were also detected.

Antimony Selenium Mixture (Molar Ratio Sb:Se = 1:1)

Examples of selected mass spectra are given in Figure 1, where identified clusters are also provided. For the ratio Sb:Se = 1:1, some Se_n^+ clusters ($n = 4$–9) and several $SbSe_n^+$ ($n = 3$–7) were detected. In addition, two oxidized clusters of $Se_6O_2^+$ and $Se_7O_2^+$ were identified. A comparison of experimental and theoretical isotopic patterns for $SbSe_2^+$ is given in Fig. S1 A, and these are in good agreement.

Antimony Selenium Mixture (Molar Ratio Sb:Se = 10:1)

Here, the mass spectra recorded from the ratio Sb:Se = 10:1 are given in Figure 2a. In addition to several Se_n^+ ($n = 4$–9) and $SbSe_n^+$ ($n = 2$–7) clusters, some other clusters such as $SbSe_nO_5^+$ ($n = 2$–6) were also detected, while the latter ones were always overlapped with $SbSe_n^+$ clusters. Also, another two $SbSe_5O_4H^+$ and $Sb_5O_7^+$ clusters are shown in the inset spectrum. Comparison of experimental and theoretical isotopic patterns demonstrating the overlap of $SbSe_3^+$ and $SbSe_2O_5^+$ clusters is shown in Fig. S1 B and there is good agreement between the experimental results and the theoretical model.

Antimony Selenium Mixture (Molar Ratio Sb:Se = 1:10)

When selenium was in high excess over antimony, the mass spectra were different (Figure 2b). In this case, $SbSe_n^+$ ($n = 2$–8), $Sb_2Se_n^+$ ($n = 1$–6), $Sb_3Se_n^+$ ($n = 1$–5), $Sb_4Se_n^+$ ($n = 1$–3) and $Sb_5Se_n^+$ ($n = 1, 2$) clusters were detected. Apart from these clusters, Se_n^+ ($n = 4$–9) clusters were also observed. Comparison of theoretical isotopic patterns corresponding to overlapping peaks of Se_8^+, $Sb_2Se_5^+$, and $Sb_4Se_2^+$ with the experimental spectrum is given in Fig. S1 C. Good agreement between the theoretical models and the experimental results was observed.

The Effect of Laser Energy (Molar Ratio Sb:Se = 1:1, Negative Ion Mode)

Spectra in the negative ion mode (Fig. S2) are different when compared to the positive ion mode. The most intensive peak is Se_4^- which contrasts with positive ion mode where Se_5^+ was the most intensive peak (cf. Figure 1). The effect of laser energy shown in this figure demonstrates that the intensity of clusters increases when laser energy goes from 90 to 100 a.u., but the mass spectra intensities decrease when the laser energy is increased to 110 a.u. A similar trend was observed for the Se_4^- cluster. Except for Se_4^-, the intensity of spectra

Table 1. Overview of Sb_mO_x and Se_nO_x Formed from Antimony or Selenium and Sb_mSe_n Clusters Formed from Antimony-Selenium Mixtures (1:1, 1:10, 10:1) via Laser Ablation in Positive Ion Mode. (Comment: Oxygen Containing Clusters are Not Given for the Antimony-Selenium Mixtures)

					only antimony				
	Sb^+ SbO^+	Sb_2^+ Sb_2O^+	Sb_3^+ Sb_3O^+	Sb_4^+ Sb_4O^+	Sb_5^+ Sb_5O^+	Sb_6^+			
					only selenium				
		Se_2^+	Se_3^+	Se_4^+	Se_5^+ $Se_5O_3^+$	Se_6^+ $Se_6O_2^+$	Se_7^+ $Se_7O_2^+$	Se_8^+ $Se_8O_2^+$	Se_9^+ $Se_9O_2^+$
m					Sb:Se = 1:1				
0				Se_4^+	Se_5^+	Se_6^+	Se_7^+	Se_8^+	Se_9^+
1		$SbSe_2^+$	$SbSe_3^+$	$SbSe_4^+$	$SbSe_5^+$	$SbSe_6^+$	$SbSe_7^+$		
					Sb:Se = 10:1				
0				Se_4^+	Se_5^+	Se_6^+	Se_7^+	Se_8^+	Se_9^+
1		$SbSe_2^+$	$SbSe_3^+$	$SbSe_4^+$	$SbSe_5^+$	$SbSe_6^+$	$SbSe_7^+$		
					Sb:Se =1:10				
0				Se_4^+	Se_5^+	Se_6^+	Se_7^+	Se_8^+	Se_9^+
1		$SbSe_2^+$	$SbSe_3^+$	$SbSe_4^+$	$SbSe_5^+$	$SbSe_6^+$	$SbSe_7^+$	$SbSe_8^+$	
2	Sb_2Se^+	$Sb_2Se_2^+$	$Sb_2Se_3^+$	$Sb_2Se_4^+$	$Sb_2Se_5^+$	$Sb_2Se_6^+$			
3	Sb_3Se^+	$Sb_3Se_2^+$	$Sb_3Se_3^+$	$Sb_3Se_4^+$	$Sb_3Se_5^+$				
4	Sb_4Se^+	$Sb_4Se_2^+$	$Sb_4Se_3^+$						
5	Sb_5Se^+	$Sb_5Se_2^+$							

grows as the laser energy increases. It is interesting to note that in both positive and negative ion modes, $SbSeO_2H_7^{+/-}$ clusters were detected (Fig. S3).

Review of Sb_mSe_n Clusters

An overview of the Sb_mSe_n clusters generated from Sb:Se = 1:1, Sb:Se = 1:10, and Sb:Se = 10:1 is given in Table 1 and Fig.

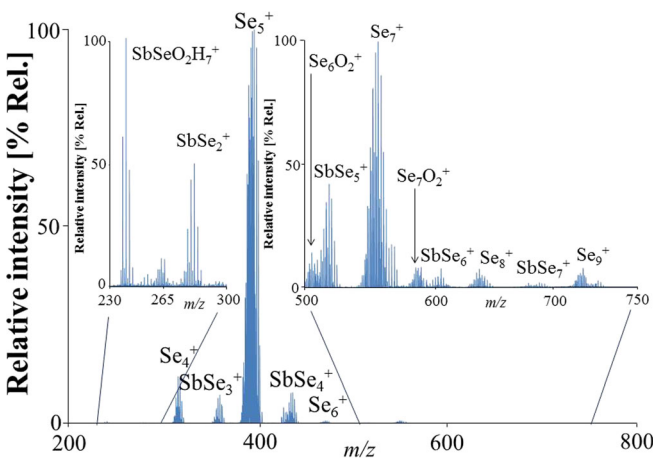

Figure 1. Mass spectra recorded from LDI of Sb:Se mixture with the ratio of elements equal to 1:1. Insets show the magnification of spectra in *m/z* ranges 230–300 and 500–750. Conditions: positive ion mode, laser energy 130 a.u

S4. Interestingly, all Sb_mSe_n clusters produced when using Sb:Se = 1:1 are also observed when Sb:Se was equal to 10:1.

Some Special Approaches to Measurement

In addition to laser ablation of the Sb-Se mixtures, some special approaches were examined.

Laser Ablation Generation in the "Hole" When the laser was fired on one point (Fig. S5) with a power from 80 a.u. to 180 a.u., there is a formation of a "*hole*" in the deposited sample material (Sb:Se = 1:1). The generation goes on in the reaction "crucible" (hole formed by the laser) and the clusters were observed at 140 a.u. (trace point). Although the intensities of clusters are low, some new Sb_2Se^+, $Sb_2Se_2^+$, Sb_3Se^+, and Sb_3^+ clusters are formed (compare to Figure 1). As the laser energy increased, the proportion of $Sb_2Se_2^+$ overlaying Se_5^+ and $Sb_2Se_2^+$ increased.

Laser Ablation Generation of Sb_mSe_n Clusters in Glycerol, Parafilm, and in Ionic Liquid When a mixture of Sb:Se = 1:1 was prepared in glycerol, laser ablation of this mixture showed the same clusters (compare with Figure 1), except for $SbSeO_2H_7^+$, $Se_6O_2^+$, and $Se_7O_2^+$ clusters (Fig. S6), but the spectra were of lower intensity.

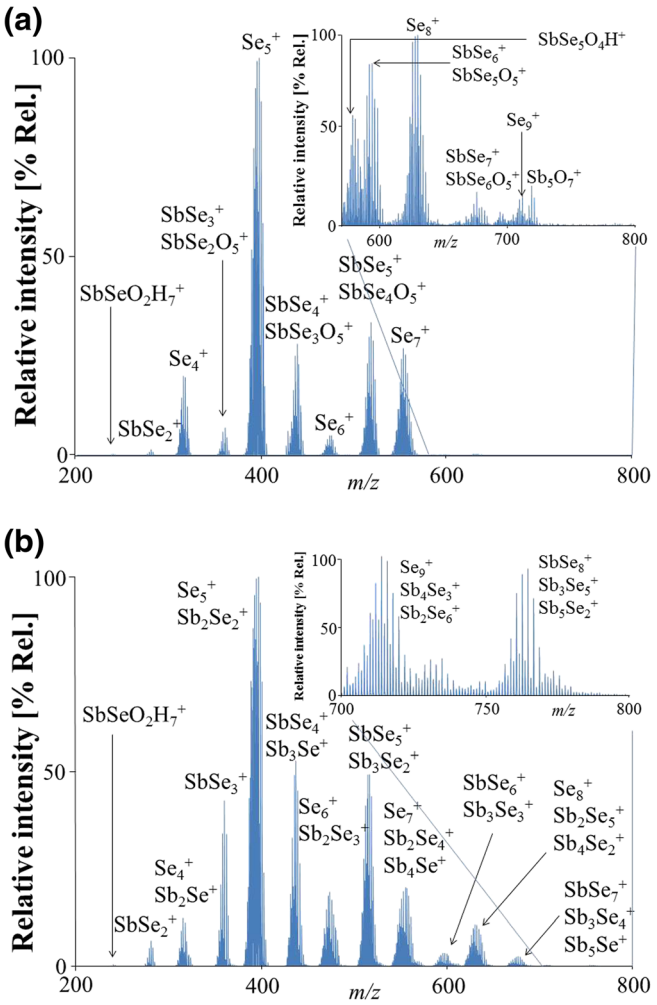

Figure 2. (**a**) Mass spectra recorded from LDI of Sb:Se mixture with the ratio of element equal to 10:1. Inset shows magnification of spectra in *m/z* range 550–800. Conditions: positive ion mode, laser energy 130 a.u. (**b**) Mass spectra recorded from LDI of Sb:Se mixture with the ratio of elements equal to 1:10. Inset shows magnification of spectra in *m/z* range 700–800. Conditions: positive ion mode, laser energy 180 a.u

When the mixture of Sb:Se = 1:1 was prepared in parafilm, the clusters produced in *m/z* range 300–600 are the same as those observed using just a 1:1 mixture (Figure 1), but they are different in *m/z* range 600–900 (Figure 3), where four clusters $Sb_3Se_n^+$ ($n = 3–6$) were generated.

When a mixture of antimony-selenium (1:1) was prepared in an ionic liquid, in comparison to Figure 1, $SbSe_3^+$ and two new clusters $Sb_2Se_2^+$ and Sb_3Se^+ were identified in the mass spectrum (Fig. S7). Some clusters were of complex overlay and were not identified.

Laser Ablation of a Commercial Sb_2Se_3 Compound

Laser desorption ionization of commercial crystalline Sb_2Se_3 shows the formation of $SbSe_2^+$, $SbSe_3^+$, $Sb_2Se_{2–4}^+$, $Sb_2Se_{3–4}^+$, and $Sb_3Se_{1–5}^+$ clusters, the same as when mixtures of Sb:Se =

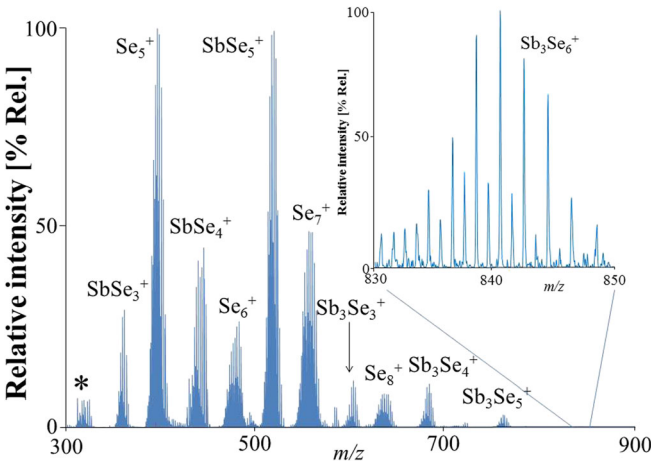

Figure 3. Mass spectra recorded from LDI of Sb:Se mixture in the parafilm with the ratio of elements equal to 1:1. Conditions: positive ion mode, laser energy 160 a.u.; asterisk (*) means that isotopic pattern is too complex or the spectra intensity is too low to identify clusters

1:10 were ablated. The only exceptions are Se_n^+ clusters. Missing Se_n^+ clusters is natural, as Se_n^+ structural fragments with Se-Se bounds are not part of Sb_2Se_3 crystal structure (Figure 4). In negative ion mode, only $SbSe_2^-$, Sb_2Se^-, $SbSe_3^-$, and $Sb_2Se_2^-$ clusters were detected.

Structure of Sb_mSe_n Clusters

Structures of some unary clusters were recently determined for selenium [12–15] and antimony [16, 17] clusters. However, structures of generated binary clusters are not known. The determination of the structures from mass spectra is not possible and quantum chemistry computation is outside the scope of this work.

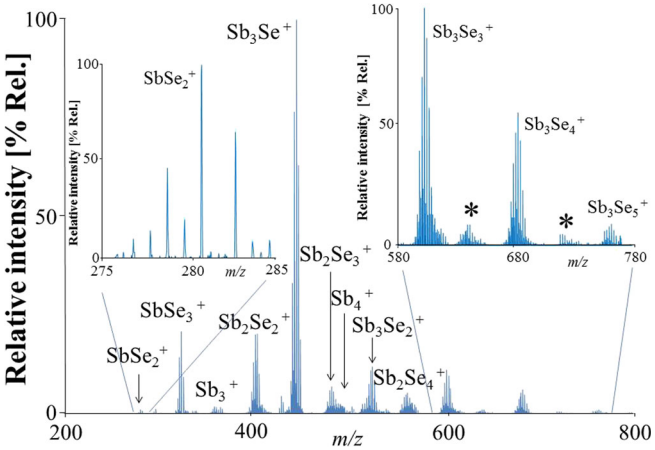

Figure 4. Mass spectra recorded from LDI of commercial Sb_2Se_3 crystals. Conditions: positive ion mode, laser energy 130 a.u.; asterisk (*) means the isotopic pattern is too complex or the spectra intensity is too low to identify clusters

Discussion

In order to understand the structures of Sb-Se chalcogenide glasses, we studied the formation of clusters generated from a mixture of Sb-Se in three different ratios and in different media. Comparing the results obtained, the clusters formed when using the ratio Sb:Se = 1:1 and 10:1 was quite similar. Contamination of $Sb_mSe_n^+$ clusters with oxidized $Sb_mSe_nO_5^+$ species was not observed for Sb:Se = 1:1 samples. This is probably because antimony is easily oxidized and thus oxidized specie was detected from samples with high excess of antimony. Therefore, when antimony was in high excess, some oxidized species like $Sb_mSe_nO_5^+$ could be produced in greater extend. The situation was different when Sb:Se = 1:10, many new $Sb_mSe_n^+$ clusters were observed which were not generated in Sb:Se = 1:1. The reason could be that selenium has a smaller atomic diameter and lower melting temperature than antimony. Therefore, when selenium is in molar excess, the selenium surrounds the antimony, and under the influence of the laser, it will melt first and combine with the antimony around it to form various clusters.

When the laser acts on one point, a "hole" will be created. Although low laser energy is not enough to form ions, chemical reactions actually took place between the elements.

Conclusions

Laser desorption ionization with quadrupole ion trap time-of-flight mass spectrometry (QIT-TOFMS) can be used as a type of efficient device to generate various Sb_mSe_n clusters. The clusters Sb_m, Se_n, and Sb_mSe_n were generated from mixtures of the elements antimony and selenium. In total, 24 new antimony selenide clusters were observed. The results obtained contribute to a deeper understanding of the preparation and structure of Sb_mSe_n materials, glasses, or various phase-change products.

Acknowledgements

This work was funded with support from the Grant Agency of the Czech Republic (Projects No. GA18-03823S). This research has been also supported by CEPLANT, the project R&D center for low-cost plasma and nanotechnology surface modification, and CZ.1.05/2.1.00/03.0086 funding by the European Regional Development Fund and the Project CZ.1.07/2.3.00/30.0058 of the Ministry of Education, Youth and Sports of the Czech Republic.

References

1. Tideswell, N.W., Kruse, F.H., McCullough, J.D.: The crystal structure of antimony selenide, Sb_2Se_3. Acta Cryst. **10**, 99–102 (1957)
2. Voutsas, G.P., Papazoglou, A.G., Rentzeperis, P.J., Siapkas, D.: The crystal structure of antimony selenide, Sb_2Se_3. Z. Kristallogr. Cryst. Mater. **171**, 261–268 (1985)
3. Vadapoo, R., Krishnan, S., Yilmaz, H., Marin, C.: Electronic structure of antimony selenide (Sb_2Se_3) from GW calculations. Phys. Status Solidi B. **3**, 700–705 (2011)
4. Deringer, V.L., Stoffel, R.P., Wuttig, M., Dronskowski, R.: Vibrational properties and bonding nature of Sb_2Se_3 and their implications for chalcogenide materials. Chem. Sci. **6**, 5255–5262 (2015)
5. Ahmed, E., Isaeva, A., Fiedler, A., Haft, M., Ruck, M.: $[Sb_{10}Se_{10}]^{2+}$, a heteronuclear polycyclic polycation from a room-temperature ionic liquid. Chem. Eur. J. **17**, 6847–6852 (2011)
6. Ahmed, E., Breternitz, J., Groh, M.F., Isaeva, A., Ruck, M.: $[Sb_7Se_8Br_2]^{3+}$ and $[Sb_{13}Se_{16}Br_2]^{5+}$- double and quadruple spiro cubanes from ionic liquids. Eur. J. Inorg. Chem. **19**, 3037–3042 (2014)
7. Wang, J., Lee, K., Kovnir, K.: Synthesis, crystal structure, and thermoelectric properties of two new barium antimony selenides: $Ba_2Sb_2Se_5$ and $Ba_6Sb_7Se_{16}$. J. Mater. Chem. C. **3**, 9811–9818 (2015)
8. Martin, T.M., Wood, P.T., Kolis, J.W.: Synthesis and structure of an $[Sb_{12}Se_{20}]^{4-}$ salt: the largest molecular zintl ion. Inorg. Chem. **33**, 1587–1588 (1994)
9. Ko, J.B., Myung, T.-S.: Structural and thermal properties of Ge-Sb-Se chalcogenide glasses for an application in infrared optical product design and manufacture. J. Ceram. Process. Res. **12**, 132–134 (2011)
10. Choi, J.H., Cha, D.-H., Kim, J.-H., Kim, H.-J.: Development of thermally stable and moldable chalcogenide glass for flexible infrared lenses. J. Mater. Res. **31**, 1674–1680 (2016)
11. Parnell, H., Butterworth, J.H., Sakr, H., Tang, Z., Furniss, D., Benson, T.M., Scotchford, C., Seddon, A.B.: Ge-Sb-Se glass fiber-optics for in-vivo mid-infrared optical biopsy. Proc. SPIE. **9703**, 970309 (2016)
12. Prokeš, L., Kubáček, P., Peña-Méndez, E.M., Amato, F., Conde, J.E., Alberti, M., Havel, J.: Laser ablation synthesis of gold selenides by using a mass spectrometer as a synthesizer: laser desorption ionization time-of-flight mass spectrometry. Chem. Eur. J. **22**, 11261–11268 (2016)
13. Hohl, D., Jones, R.O., Car, R., Parrinello, M.: The structure of selenium clusters - Se_3 to Se_8. Chem. Phys. Lett. **139**, 540–545 (1987)
14. Xu, W., Bai, W.: The selenium clusters Se_n (n = 1–5) and their anions: structures and electron affinities. J. Mol. Struc.-THEOCHEM. **854**, 89–105 (2008)
15. Alparone, A.: Density functional theory Raman spectra of cyclic selenium clusters Se_n (n = 5–12). Comput. Theor. Chem. **988**, 81–85 (2012)
16. Geusic, M.E., Freeman, R.R., Duncan, M.A.: Neutral and ionic clusters of antimony and bismuth: a comparison of magic numbers. J. Chem. Phys. **89**, 223–229 (1988)
17. Zhai, H.-J., Wang, L.-S., Kuznetsov, A.E., Boldyrev, A.I.: Probing the electronic structure and aromaticity of pentapnictogen cluster anions Pn^{5-} (P*n* = P, As, Sb, and Bi) using photoelectron spectroscopy and ab initio calculations. J. Phys. Chem. A. **106**, 5600–5606 (2002)